THEORETICAL AND NUMERICAL STUDY ON PLASMON-ASSISTED CHANNELING INTERACTIONS IN NANOSTRUCTURES

Young-Min Shin, Department of Physics, Northern Illinois University, Dekalb, IL, 60115, USA
also at Fermi National Accelerator Laboratory (FNAL), Batavia, IL 60510, USA

Abstract

A plasmon-assisted channeling acceleration can be realized with a large channel possibly at the nanometer scale. Carbon nanotubes are the most typical example of nano-channels that can confine a large amount of channeled particles and confined plasmons in a coupling condition. This paper presents a theoretical and numerical study on the concept of laser-driven surface-plasmon (SP) acceleration in a carbon nanotube (CNT) channel. An analytic description of the SP-assisted laser acceleration is detailed with practical acceleration parameters, in particular with specifications of a typical tabletop femto-second laser system. The maximally achievable acceleration gradients and energy gains within dephasing lengths and CNT lengths are discussed with respect to laser-incident angles and CNT-filling ratios.

INTRODUCTION

Laser accelerations based on photon-matter interactions typically take advantage of intense driving lasers with excessively high power at the level of Tera-watt or even Peta-watt to quickly ionize a gas target (or often solid targets) and to raise particle energies to the MeV scale. Such femto-second laser systems occupy a large physical space, while the acceleration medium/target itself is relatively much smaller than the driving source, and, in spite of their exceptionally large field strengths, downside of using a solid target for the laser-acceleration is that the targets become vulnerable to intense laser-matter interactions and could be readily destroyed under the impact of a short pulse driving source. The system size and limited reproducibility have refrained laser-accelerations from being adapted to accelerator-based systems. It would be more practical to increase laser-target coupling efficiency and/or repetition rate, while keeping the laser intensity sufficiently low, perhaps below the target ionization threshold. In particular, affordable laser intensities would be more compatible with systems in practically applicable sizes. In such a way, structuring a target can improve the acceptance of channeling particles and field confinements in the acceleration region, which would increase laser-plasma coupling efficiency. A CNT, synthetic nanostructure consisting of honeycomb unit cells based on *sp*-2 carbon-bonding, is well suited for laser-driven acceleration since oscillatory plasma waves (SPs) are readily generated by a photo-excitation in such a structured negative index material [1, 2]. If the optical wavelength of a driving laser is close enough to a plasma wavelength of the CNTs, the laser would strongly perturb a density state of conduction electrons on the tube and excite surface plasmons at the photon-plasmon coupling condition. The optical properties and coupling condition can be effectively controlled by CNT parameters such as the diameter and aerial density. In this condition, it is regarded that the laser is coupled into an effective metallic substrate with homogenized optical parameters (plasma frequency, permittivity, refractive index, and absorption coefficient) that are averaged over an area of the laser wavelength on a target implanted with sub-wavelength CNTs.

SYSTEM DESCRIPTION

Figure 1 depicts the concept of the laser-driven SPP acceleration in a nanotube. In the substrate target, particles channeled in the nanotube are repeatedly accelerated and focused by confined fields of the laser-excited SPP along the CNTs embedded in the nano-holes under the phase-velocity matching condition. The energy gain of accelerated particles, if any, is limited by the dephasing length. Continuous phase velocity matching between particles and SP waves can be extended by tapering the longitudinal plasma density in a target. In a CNT-target, the longitudinal plasma density profile can be controlled by selectively adjusting tube dimensions. When an intense short pulse laser illuminates the near-critical density plasma, the inductive acceleration field moves with a speed v_g, which is less than v_p, depending on the plasma density: $v_g = c\sqrt{1 - \omega_p^2/\omega^2}$, where c is the speed of light, ω_p is the electron plasma frequency, and ω is the laser frequency. The accelerating ions have a progressively higher speed along the targets, so the inductively accelerated ions are kept accelerating for a long time inside the near-critical density plasma target. The distance between the two adjacent targets are also adjusted accordingly.
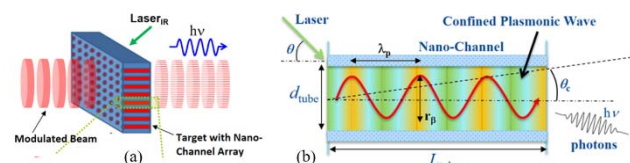
Figure 1: (a) Conceptual drawing of laser-pumped CNT-acceleration and (b) photo-excited plasmonic wave interacting with CNT-channelling electrons.

The acceleration mechanism of the laser-excited sub-λ plasmon is conceptually depicted in Fig. 1, illustrating accelerating particles in a laser-pumped CNT channel [3, 4]. The laser irradiated on a target modulates the electron density of the CNT and quickly induce a plasma oscillation at a photon-plasmon coupling condition. The photo-excited density fluctuation induces electromagnetic fields in a

3: Advanced Acceleration Techniques and Alternative Particle Sources

A16 - Advanced Concepts

CNT and the oscillating evanescent fields penetrate in the tube within the attenuation length. The charged particles channeling through a tube are accelerated by the induced SPPs at their phase-matching condition. The energy gain remains until the particles begin to outrun the plasma wave and are dephased from the SPP. A proper target thickness would therefore be mostly determined by the dephasing length if there is no additional phase-matching mechanism implemented in the single target acceleration. Accelerating parameters of a sub-wavelength CNT accelerator are outlined in more details with typical specifications of a tabletop femto-second laser in the next section.

THEORETICAL MODEL

An effective density of electron plasma over multi-walled CNTs is mostly controlled by tube diameter, number of walls, and spacing between the tubes in a unit area ($\sim\lambda_L^2$). The lattice constant of carbon-bonding in a honey-comb unit cell on a CNT wall is $a_0 \sim 1.4$ Angstrom and wall-to-wall spacing is normally $d = 3.4$ Angstrom. A local tube wall density is about 8×10^{22} cm^{-3} and a typical diameter of CNT ranges up to a few hundred nanometers, which is usually related to the tube length. Given that a single CNT is sized from a few tens of nanometer up to 1 μm in diameter, which would be effectively the same as a few hundred square nanometers to a few square microns of unit area on a target, the effective electron plasma density averaged over a volume of CNT ranges from $10^{21} - 6 \times 10^{23}$ e^-/cm^3. The density corresponds to $10^{20} - 10^{22}$ e^-/cm^3 over a CNT-embedded unit area ($\sim \lambda_L^2$), as depicted in Fig. 1.

In the given condition, a CNT channel can be described by a homogenized model with effective dielectric parameters. Let us consider an array of parallel nanotubes of areal density N_c, with axes parallel to z (Fig. 2 (b), inset). The separation between the nanotubes is $d = N_c^{-1/2}$, the free electron density inside a nanotube is n_0, and the tube radius is r_c. A nanotube can be treated as a superposition of overlapping cylinders of free electrons and immobile ions. The dispersion/absorption relation of the periodic array is given by $\kappa = k_r + ik_i$, where

$$k_r(\omega) = \frac{\omega}{c}\sqrt{\frac{\left(\varepsilon_L - \frac{\omega_p'^2}{\omega^2 - \omega_p^2/2}\right)\left(\varepsilon_L - \frac{\omega_p'^2}{\omega^2 - \omega_p^2}\right)}{\varepsilon_L - \left(\omega_p'^2/\omega^2 - \omega_p^2\right)\left(\cos^2\theta + \frac{\omega^2}{\omega^2 - \omega_p^2/2}\sin^2\theta\right)}} \quad (1)$$

and

$$k_i(\omega) = \frac{\omega^3 v \omega_p'^2}{2c^2(\omega^2 - \omega_p^2)^{3/2} k_r}\left(\frac{\varepsilon_L - \frac{\omega_p'^2}{\omega^2 - \omega_p^2/2} + \left(\varepsilon_L - \frac{\omega_p'^2}{\omega^2 - \omega_p^2}\right)\frac{(\omega^2 - \omega_p^2)^2}{(\omega^2 - \omega_p^2/2)^2}}{\varepsilon_L - \frac{\omega_p^2}{\omega^2 - \omega_p^2}\left(\cos^2\theta + \frac{\omega^2 - \omega_p^2}{\omega^2 - \omega_p^2/2}\sin^2\theta\right)} - \frac{\left(\varepsilon_L - \frac{\omega_p'^2}{\omega^2 - \omega_p^2/2}\right)\left(\varepsilon_L - \frac{\omega_p'^2}{\omega^2 - \omega_p^2}\right) + \left(\cos^2\theta + \frac{(\omega^2 - \omega_p^2)^2}{(\omega^2 - \omega_p^2/2)^2}\sin^2\theta\right)}{\left(\varepsilon_L - \frac{\omega_p^2}{\omega^2 - \omega_p^2}\left(\cos^2\theta + \frac{\omega^2 - \omega_p^2}{\omega^2 - \omega_p^2/2}\sin^2\theta\right)\right)^2}\right) \quad (2)$$

Here, $\omega_p = \sqrt{\frac{n_e e^2}{\varepsilon_0 m}}$, $n_e = Zn_0$, and $\omega_p'^2 = s\omega_p^2$ (n_0 is the ion

density of a single CNT and $s = \pi r_r^2/d^2$ is the aerial CNT-filling ratio). For $\varepsilon_L = 5.5$ (for graphite), $n_e = 10^{21}$ cm^{-3}, $r_c = 50$ nm, and $d = 150$ nm, $\pi r_c^2 N_c \sim 0.35$, and $v/\omega_p \sim 0.001$, the dispersion/absorption relations of a CNT-confined SPP with respect to p-polarized laser is plotted in Fig. 2.
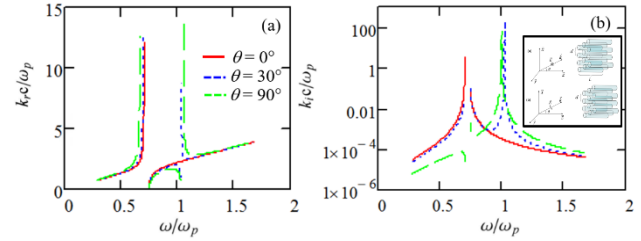
Figure 2: Normalized (a) dispersion (k_r) and (b) absorption (k_i) graphs of the laser-excited SPP in a CNT array (Inset: schematic of laser propagation through an array of carbon nanotubes. (top) laser polarization k ∥ y (s-polarization) and (bottom) laser polarization in the x–z plane (p-polarization).).

It is apparent that confined modes are excited at the harmonic SPP-coupling conditions with the light line (laser photon). At the resonance condition, the laser-light is thus coupled into the sub-wavelength CNT and the plasma density of the SPP is modulated with the laser wavelength ($\lambda_L = \lambda_p > r_{cnt}$, where r_{cnt} is the radius of CNT). The laser-excited SP wave moves along the tube within the absorption length and subsequently forms a standing plasma wave (plasma oscillation) when the photon-plasmon energy transfer reaches the equilibrium. With a sufficiently narrow energy spread, the particles channeled in the tube, if simultaneously injected into the CNTs during the excitation, can be accelerated by the evanescent fields confined in the sub-λ CNT at the phase-velocity matching condition.

If the laser beam is coupled into the CNT array with an incident angle, θ, then the electric field of p-polarized laser beam is $\vec{E}_L = \hat{x}E_x + \hat{z}E_z$ where $E_x = A_x e(x,z)$ and $E_z = A_z e(x,z)$ ($A_x = A_0 \sin\theta$ and $A_x = A_0 \cos\theta$). At the laser-SP coupling condition, the electron plasma density of a nanotube modulated by the laser-excited SP is defined as

$$n_e = Zn_0\left(1 + a_0 e^{-\frac{r^2}{2r_s^2}}\right)^{-2} e^{i(\kappa z - \omega_{laser}t)} \quad (3)$$

where

$$a_0 = \frac{eA_0 \cos\theta \cdot \sqrt{s}}{m(\omega_{laser}^2 - \omega_p^2/2)r_c} \quad (4)$$

Also, the SP has the electric field components

$$E_x = \frac{Zn_0 e}{\varepsilon_0}a_0 \xi e^{-\frac{r^2}{2r_s^2}} e^{i(\kappa z - \omega_{laser}t)}\cos\theta_{CNT} \quad \text{and}$$

$$E_z = \frac{Zn_0 e}{\varepsilon_0}a_0 \xi e^{-\frac{r^2}{2r_s^2}} e^{i(\kappa z - \omega_{laser}t)}\sin\theta_{CNT} \quad (5)$$

where ξ is the distance from the tube axis and θ_{CNT} is the refraction angle of the transmitted wave in the substrate,

3: Advanced Acceleration Techniques and Alternative Particle Sources

A16 - Advanced Concepts

defined as $\theta_{CNT} = \sin^{-1}\left(\dfrac{\sin\theta}{n_{CNT}}\right)$. Here, $n_{CNT} = \dfrac{k_r}{\omega_{laser}/c}$, where k_r = $k_r(\omega = \omega_{laser})$. The electric fields averaged over the tube radius, r_c, therefore, are

$$\langle E_x \rangle = \frac{1}{r_c}\int_0^{r_c} E_x(\xi)d\xi = \frac{Zn_0 e}{2\varepsilon_0} a_0 r_c e^{-\frac{r^2}{2r_s^2}} e^{i(\kappa z - \omega_{laser}t)}\cos\theta_{CNT} \tag{6}$$

and

$$\langle E_z \rangle = \frac{1}{r_c}\int_0^{r_c} E_z(\xi)d\xi = \frac{Zn_0 e}{2\varepsilon_0} a_0 r_c e^{-\frac{r^2}{2r_s^2}} e^{i(\kappa z - \omega_{laser}t)}\sin\theta_{CNT} \tag{7}$$

Note that the averaged fields have no dependence upon the tube radius. The transverse field $\langle E_x \rangle$ and longitudinal one, $\langle E_z \rangle$ act on focusing and accelerating the ions channeling through a nanotube at the phase-velocity matching condition respectively. The energy gain of accelerated ions along the CNT is given by integrating $\langle E_z \rangle$ over acceleration length as follows,

$$W_z = \left(\frac{Zn_0 e}{2\varepsilon_0}\right)\left(a_0 r_c e^{-\frac{r^2}{2r_s^2}}\right)\left(\frac{1-e^{-k_i z}}{k_i}\right)\sin\theta_{CNT} \tag{8}$$

Figure 3 (a)/(b) shows axial distributions of the normalized plasma density and electric fields with $\theta = 50°$ and $n_0 = 3.2 \times 10^{20}$ cm^{-3} ($Z = 6$, n_e ($r = 0$, $z = 0$, and $t = 0$) $= 2 \times 10^{21}$ cm^{-3}) and 4.9 % of CNT-aerial filling ratio.
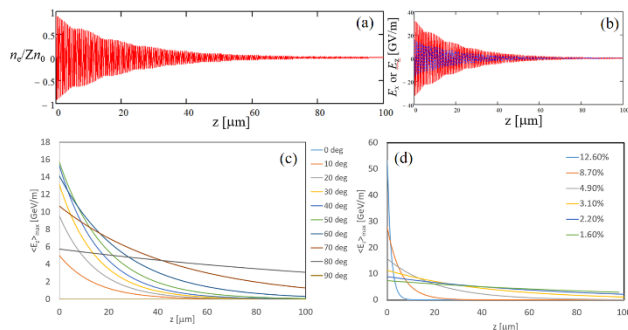
Figure 3: (a) Normalized electron plasma density and (b) electric field amplitudes ($\langle E_x \rangle$: red, $\langle E_z \rangle$: blue) versus distance (z) graphs (c) Acceleration field ($\langle E_z \rangle_{max}$) versus distance ($z$) graphs with respect to (d) incident angle (θ_{in}) ($s = 4.9$ %) and (b) aerial CNT-filling ratio (with $\theta_{in} = 50°$).

Figure 3(c)/(d) shows the maximum electric field ($\langle E_z \rangle_{max}$) in distance over a tube under two various laser-SPP coupling conditions with parametric scans on incident angles (with $s = 4.9$ %) and aerial CNT-filling ratios (with $\theta_{in} = 50°$). The peak field reaches 60 GeV/m with the large filling ratio, while steeply attenuating with distance. The field modestly attenuates with a smaller filling ratio, although the peak field drops to 5 – 6 GeV/m (over $\theta_{in} = 50 – 60$ degree). Figure 4 shows energy gain versus laser incident angle of channeling particles through a nanotube in a unit area on a substrate with respect to the aerial CNT-filling ratio (s). The ions phase-matched with the confined SPP field are accelerated by the longitudinal field until they overrun the plasma wave. According to laser-plasma acceleration theory, the dephasing length along the unit

volume across the substrate is given by $L_d = \dfrac{\lambda_p^3}{\lambda_{laser}^2}$ where $\lambda_p = \dfrac{2\pi c}{\omega_p}$ and $\lambda_{laser} = \dfrac{2\pi c}{\omega_{laser}}$. The energy gain over a dephasing length becomes maximum (0.12 MeV) at $s = 8.7$ % and $\theta_{in} = 60$ deg. The energy gain is fairly limited by the dephasing length: the particles are too rapidly kicked up and pushed away from the plasma wave by the large electric field before being fully synchronized with the SP. The particles could be continuously accelerated if they remain synchronized with the plasma wave. The continuous phase-matching condition is normally established by tapering the plasma density. Within a realistic scale of femto-second laser system, the highest laser power is limited within 100 – 125 GW and the most obtainable energy gain over a 100 μm thick target implanted with CNT array ($r_c = 50$ nm and $s = 3.1$ %) will be 0.5 – 0.6 MeV with a laser system with 125 GW, $\lambda_{laser} = 1.054$ μm, and $r_{laser} = 380$ μm, corresponding to 5 – 6 GeV/m gradient.
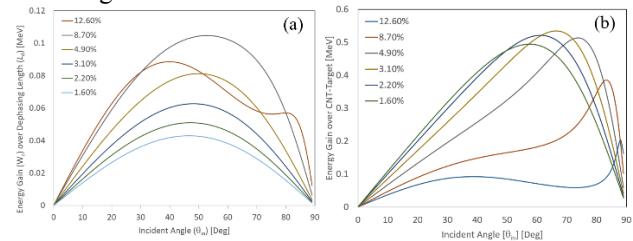
Figure 4: Energy gain (W_z) versus incident angle (θ_{in}) over (a) dephasing length and (b) CNT-implanted target ($z = 100$ μm) with respect to aerial CNT-filling ratio (s).

CONCLUSION

In conclusion, multiwall CNTs embedded in a template play a role in an effective plasma channel that can confine SP waves with intense focusing and accelerating fields of order GV/m, below the ablation threshold. A laser-excited sub-wavelength plasmon field is capable of accelerating charged particles guided in the channel up to sub-MeV in the dephasing length and MeV in an affordable CNT length.

ACKNOWLEDGEMENT

REFERENCES

[1] Wei Zhang, Huagang Xiong, Shaokai Wang, Min Li, and Yizhuo Gu, *Appl. Phys. Lett.* 106, 182905, 2015.

[2] Xiuchao Yao, Xuechen Kou, Jun Qiu and Mark Moloney, *RSC Advances* Issue 42, 2016, to be published.

[3] Young-Min Shin, *APL* 105, 114106, 2014.

[4] Y. M. Shin, *et. al.*, *POP* 20, 123106, Dec., 2013.